Textures and Microstructures, 1986, Vol. 6, pp. 231–254
0730–3300/86/0604–0231 $18.50/0

Printed in the United Kingdom

Evaluation of the Effect of Initial Texture on the Development of Deformation Texture

T. LEFFERS and D. JUUL JENSEN
Metallurgy Department, Risø National Laboratory, DK-4000 Roskilde, Denmark

(Received May 5, 1986)

We describe a computer procedure which allows us to introduce experimental initial textures as starting conditions for texture simulation (instead of a theoretical random texture). We apply the procedure on two batches of copper with weak initial textures and on fine-grained and coarse-grained aluminium with moderately strong initial textures. In copper the initial texture turns out to be too weak to have any significant effect. In aluminium the initial texture has a very significant effect on the simulated textures—similar to the effect it has on the experimental textures. However, there are differences between the simulated and the experimental aluminium textures that can only be explained as a grain-size effect. Possible future applications of the procedure are discussed.

INTRODUCTION

It is obvious and well established that a strong initial texture can have a decisive effect on the development of deformation texture. For instance, Sundberg (1968) has shown that aluminium with a special strong initial texture ($\{211\}\langle 011\rangle$) develops a rolling texture similar to the brass-type texture, and Leffers (1969a) has demonstrated that this is a natural consequence of the normal models for the formation of rolling texture.

On the other hand, the effect of weak or moderately strong initial textures on the development of deformation texture has not been investigated in detail—in spite of the fact that this effect may be quite important for the investigation of the early stages of texture formation. Exactly the investigation of the early stages of texture development is one of the more promising paths for the progress in texture research, because it is relatively easy to make microstructural investigations to supplement the texture measurements at this stage.

The typical problem to be dealt with in connection with the effect of initial texture is the following. We observe an anomaly in texture development in a material with non-random starting texture or a difference in texture development between similar materials with different starting textures, and we want to know whether the anomaly/difference is caused by the starting texture(s) or by some other characteristic of the material(s).

The obvious way of dealing with this problem is to introduce the experimentally measured orientation distribution function (ODF) of the starting materials in the normal computer models for texture formation (assuming that we have reasonable good "normal" models for the formation of deformation texture in initially texture-free materials)—and then compare the resulting calculated textures with those observed experimentally. If the calculated and the experimental texture agree, the observed effect is a trivial consequence of the initial texture. If they do not agree, the observed effect is caused by some special characteristic of the materials—or it is a non-trivial effect of the initial texture (see discussion section).

In the present work we describe a system of computer programs which performs the above task of introducing the initial experimental texture as starting condition for texture simulation which, in turn, produces calculated textures for comparison with the textures developed in the experiments. We quote two cases as illustrations of the application of the computer procedure: the early stage of the development of rolling texture in two batches of copper with different weak initial textures and the early stage of the development of rolling texture in coarse-grained and fine-grained aluminium with similar, but not identical, moderately strong initial textures.

THE COMPUTER PROCEDURES

Digitization of the initial texture

As "starting material" for texture simulation we generate a polycrystal consisting of a discrete number of grains (normally ~10,000) with an orientation distribution which represents the ODF of the real starting material. In the generation of this orientation distribution a representative section of orientation space (subspace III, Hansen, Pospiech and Lücke, 1978) is subdivided into a number of areas (1800), each area being characterized by one (experimental) orientation density. From this orientation density and the volume fraction of orientation space the area represents, we calculate the fraction of the grains which should have their orientation in the considered area. This fraction multiplied by the total number of grains we want to generate gives the "ideal" number of grains in the area. As a first step a number of orientations, equal to the integer nearest below the ideal number, are generated in random distribution in the area considered. In the next step we arrange the areas in groups of 8 (or as close as possible to 8), and in each group we generate a randomly distributed number of orientations equal to the integer closest to the sum of the differences between the 8 ideal numbers and the integer numbers of orientations already generated. In this way we get a discrete number of grains with an orientation distribution close to that of the material considered.

In all cases to be reported we aimed at generating 10,000 grains. Already because of the rounding-off errors we cannot expect to get exactly 10,000. We actually always got numbers slightly above 10,000—because the ODFs have some negative components, which we neglect, and correspondingly have too high positive components (for the determination of ODFs see experimental section).

combination of relaxed constraints. The program also includes a "random stress" procedure which simulates the interaction between neighbouring grains; as practically all other models this model considers the grains one by one, and therefore the interaction with the surrounding grains with their specific orientations can only be introduced as a random effect. The random stresses produce a certain deviation from Taylor's minimum-shear criterion for the selection of operative slip systems (Taylor, 1938), but they do not interfere with the fulfilment of strain continuity (Leffers, 1973). As described in detail in an earlier work (Leffers, 1975) the average magnitude of the random stresses relative to the "average stress"† may be derived in a rational way from the deformation pattern in the computer. In practice the main effect of the random stresses is to smear out the texture. In the present work we are not attempting to perform a detailed analysis of the deformation pattern. We therefore adopt a rather pragmatic attitude to the parameters of the random stress procedure (as to the other adjustable parameters of the model): we use them for curve fitting (see results section).

When comparing experimental and simulated textures, one must bear in mind that the Taylor model does not provide an unambiguous selection of slip systems, and hence it does not determine the texture development unambiguously. However, as already described by Kallend and Davies (1972), the actual selection of slip systems within the framework of the Taylor model is not very critical for the resulting simulated textures. With relaxed constraints, as mainly used in the present work, the ambiguity in texture development is further reduced. The selection of slip systems in our texture-simulation program is determined by the structure of the program and the random stresses as described in details by Leffers (1973).

The program can plot quantitative pole figures for the simulated texture ({111}, {200} and {220} pole figures) directly (without going via the ODF). In order to construct a calculated pole figure we subdivide the (quarter) pole figure into a number of areas (~300) and count the number of poles in each area. The resulting discontinuous distribution of pole densities is transformed to a

† The average stress for rolling may be taken as a tensile and a compressive stress of equal magnitude in the rolling and the normal direction, respectively.

continuous distribution for which contour lines are plotted. We have found that comparison of such calculated pole figures with experimental pole figures gives a very sensitive indication of the similarity or dissimilarity of calculated and experimental textures, and this is the approach to be adopted.

Figure 1 illustrates the operation of the procedures for the generation of pole figures from discrete orientations—and the operation of the procedure for the generation of a number of discrete orientations from an experimental ODF. The code for the pole densities is given in Table I. The figure shows the experimental {200} pole figure for fine-grained aluminium before deformation (for details see experimental section) together with the computer-generated pole figure for the computer-generated distribution of discrete orientations for this material. It is clear that the distribution of discrete orientations is an adequate representation of the experimental texture.

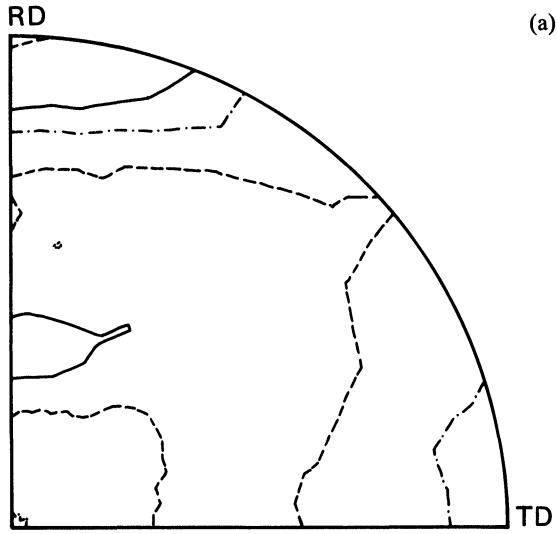

FIGURE 1 {200} pole figures for fine-grained aluminium; (a) experimental pole figure, (b) pole figure for the distribution of 11105 discrete orientations generated from the experimental ODF.

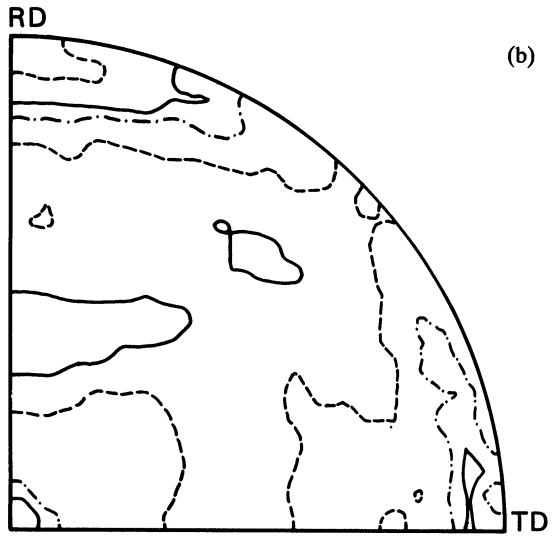

FIGURE 1 (*continued*)

TABLE I
Codes for contour lines in the pole figures

Pole densities			
Figure 18	Figure 19	All other figures	Code
0.5	0.5	0.5	solid line
1.0	1.0	1.0	dashed
2.0	2.0	1.5	dot-and-dash
3.0	3.0	2.0	full
5.0	5.0	3.0	dashed
7.0	7.0	4.0	dot-and-dash
13.0	19.0	6.0	solid

EXPERIMENTAL TEXTURES

Materials

The copper materials were produced from two batches of copper of purity better than 99.95%. Both materials were exposed to a dual

deformation/recrystallization process after casting. Copper I was rolled to 20% reduction and recrystallized at 550°C and then again rolled to 20% reduction and recrystallized at 550°C. Cu II was rolled to 48% reduction and recrystallized at 550°C and then rolled to 20% reduction and recrystallized at 550°C. The heat treatments were made in different furnaces with different heating rates which, together with the difference in reduction and the possible difference in chemical composition, would be responsible for the difference in initial texture. Copper I has a reasonably homogeneous grain-size distribution with an average grain size of 0.035 mm; copper II has a rather inhomogeneous grain-size distribution with a very small grain size (~0.015 mm) for the major fraction of the material. The aluminium materials (Hansen, Bay, Juul Jensen and Leffers, 1985) were of commercial purity (99.6%). After an initial heat treatment at 600°C for 24 h, a fine-grained starting material was produced by rolling to 50% reduction and annealing for 1 h at 350°C, and a coarse-grained starting material was produced by rolling to 20% reduction and annealing for 1 h at 400°C. The grain size of the two materials was 0.05 mm and 0.3 mm, respectively.

Texture measurements

{111}, {200} and {220} pole figures were measured by neutron diffraction and the corresponding ODFs were synthesized, using the series expansion method (Bunge, 1969) without ghost correction. For details the reader is referred to earlier work (Juul Jensen and Kjems, 1983, Juul Jensen, Hansen, Kjems and Leffers, 1984).

As already mentioned we shall use the pole figures for the comparison of experimental and simulated textures. However, we shall first describe the experimentally observed texture development in terms of ODFs.

Texture development as observed

Figure 2 shows the starting textures in Cu I and Cu II. The two textures are clearly different, but they are both rather weak. After moderate rolling reductions (40% for Cu I and 37% for Cu II) the ODFs for the two materials (not to be shown) are quite similar.

Figure 3 shows the starting textures for the fine-grained and the

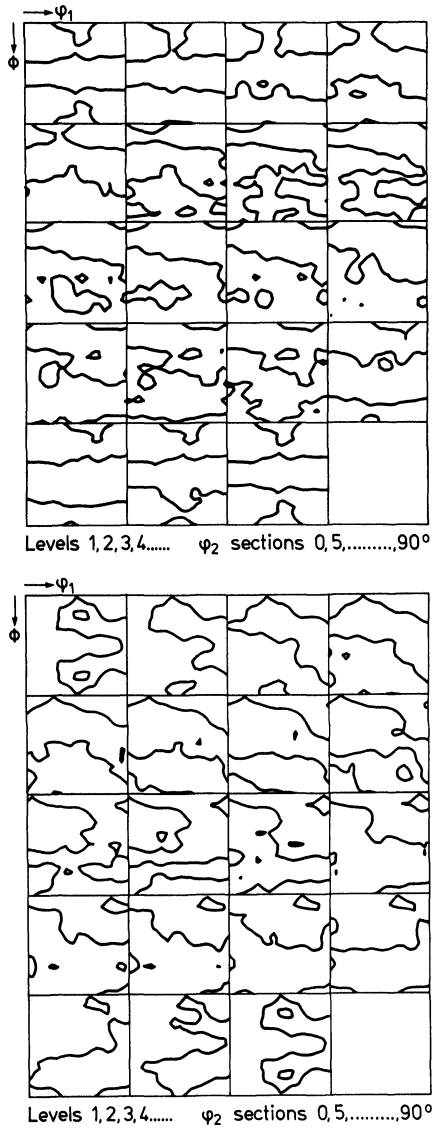

FIGURE 2 Experimental starting textures for the copper materials as represented by the ODFs; (a) Cu I, (b) Cu II.

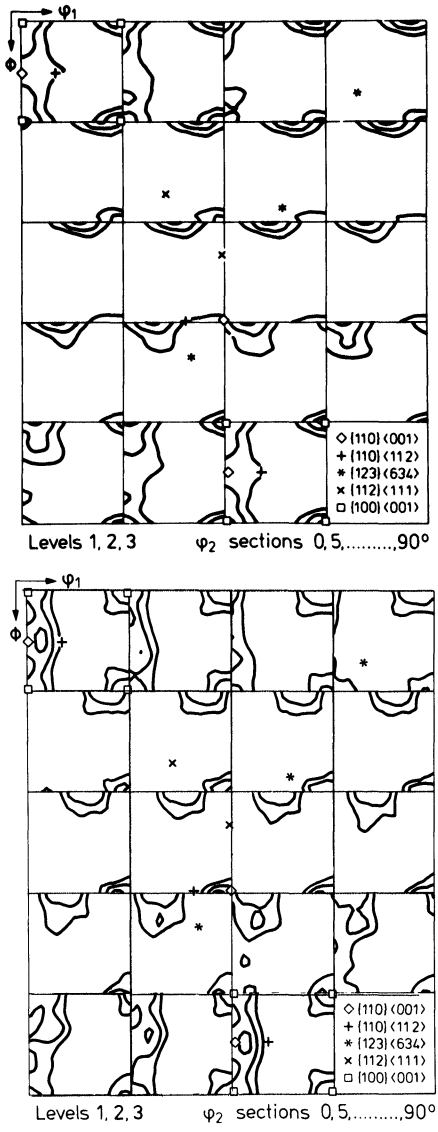

FIGURE 3 Experimental starting textures for the aluminium materials as represented by the ODFs; (a) fine-grained material, (b) coarse-grained material.

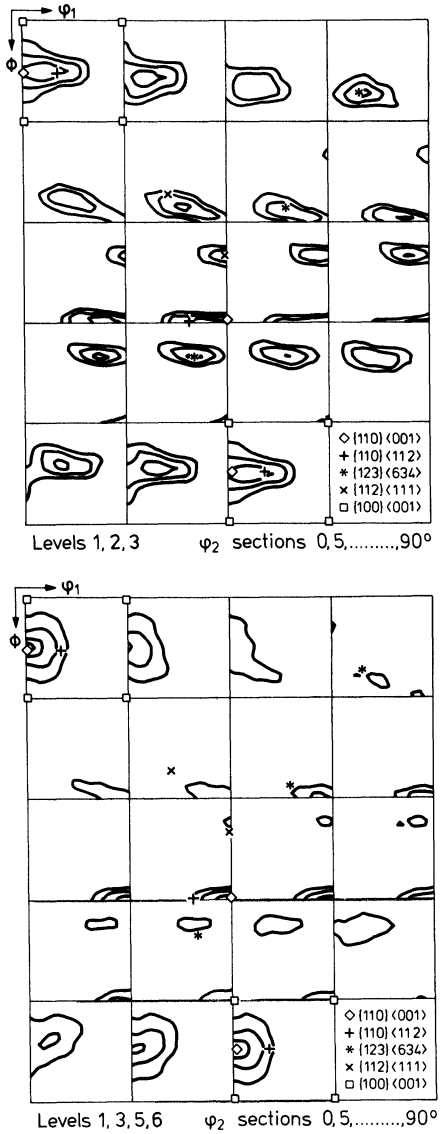

FIGURE 4 Experimental rolling textures for the aluminium materials after 50% reduction as represented by the ODFs; (a) fine-grained material, (b) coarse-grained material.

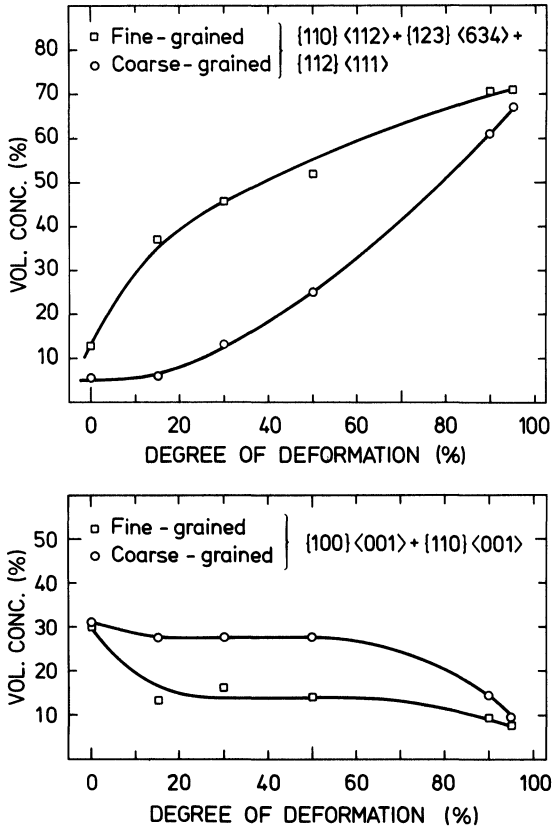

FIGURE 5 Experimentally observed texture development in the aluminium materials as represented by the changes in volume fraction of some characteristic texture components; (a) "rolling texture" (from Hansen *et al.*, 1985), (b) cube texture plus Goss texture.

coarse-grained aluminium. The two textures are similar but not identical. They both have a moderately strong fibre component with ⟨100⟩ parallel to the rolling direction. Figure 4 shows the textures after 50% rolling reduction; there is now a very clear difference between the texture of the fine-grained and the coarse-grained material. With increasing reduction the textures of the two materials become increasingly similar, and at 95% reduction there is only a rather small difference. Figure 5 shows the development in volume fraction of rolling texture as characterized by the sum of

three specific components (orientations within 15° from {110}⟨112⟩, {123}⟨634⟩ and {112}⟨111⟩) and in added volume fractions of cube and Goss texture (orientations within 15° from {100}⟨001⟩ and {110}⟨001⟩), which is a crude representation of the ⟨100⟩ fibre texture. It is clear that the formation of the rolling texture and the disappearance of the cube plus Goss texture is delayed in the coarse-grained material relative to the fine-grained material.

COMPARISON OF EXPERIMENTAL AND SIMULATED TEXTURES

The texture-simulation model contains a number of adjustable parameters: the combination of Taylor constraints, the average magnitude of the random stress components and the number of deformation steps for which a given random stress component is allowed to operate before a new component is generated. As already mentioned we shall adopt an empirical attitude and find the parameter combination which produces the best fit to the experimental texture without going into any detail discussion of the underlying theory.

In order to restrict the number of parameter combinations we have limited the number of combinations of Taylor constraints to the two normally considered for the copper-type rolling texture, viz. full constraint, FC, and one constraint relaxed, RC (ε_{31} is not forced to be zero, x_1 being the rolling direction and x_3 being the normal direction). We do not attempt to perform a transition from FC to RC conditions as suggested for instance by Tome, Canova, Kocks, Christodoulou and Jonas (1984); with our focus on relatively low strains we would actually largely remain in the FC range with the transition criteria used by Tome *et al.*

Copper material

In Figures 6–8 we present the experimental {111} and {200} pole figures for Cu I and the corresponding computer-simulated pole figures for the RC and the FC mode. The random stress parameters used in Figures 7–8 are those which produce the best fit to the experimental pole figures. However, the exact values of these

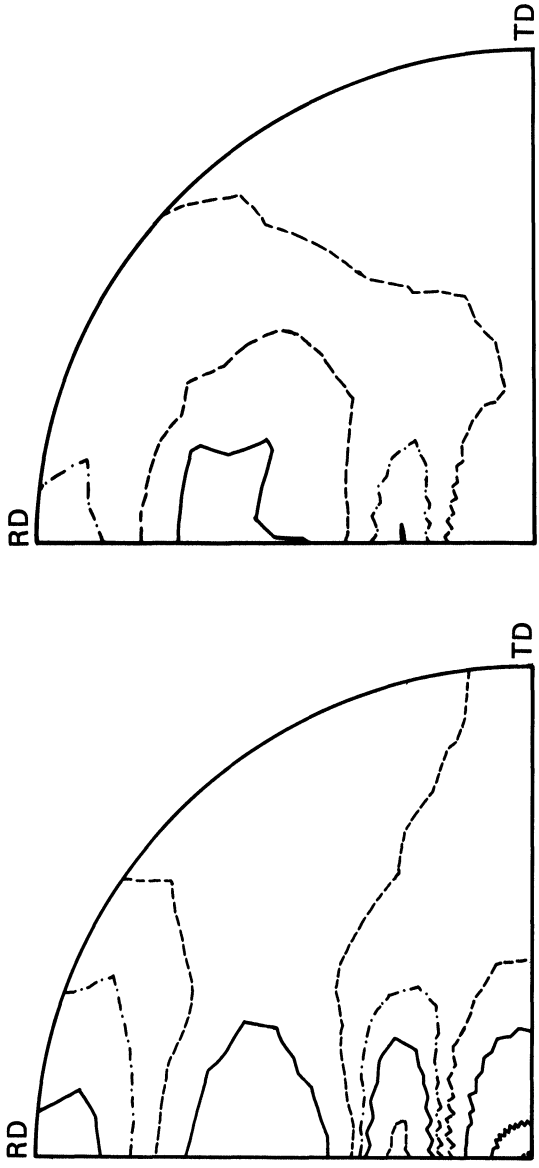

FIGURE 6 Experimental {111} and {200} pole figures for Cu I rolled to 40% reduction.

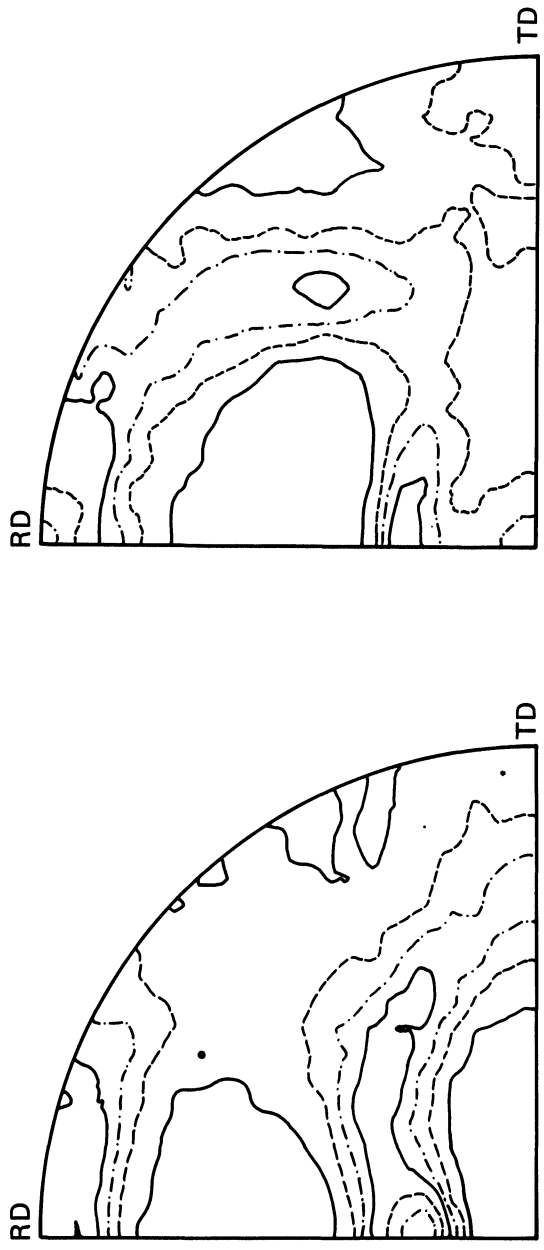

FIGURE 7 Pole figures corresponding to those in Figure 6, simulated with the RC mode starting with an orientation distribution representing the starting texture of Cu I. Reduction 40% as in Figure 6.

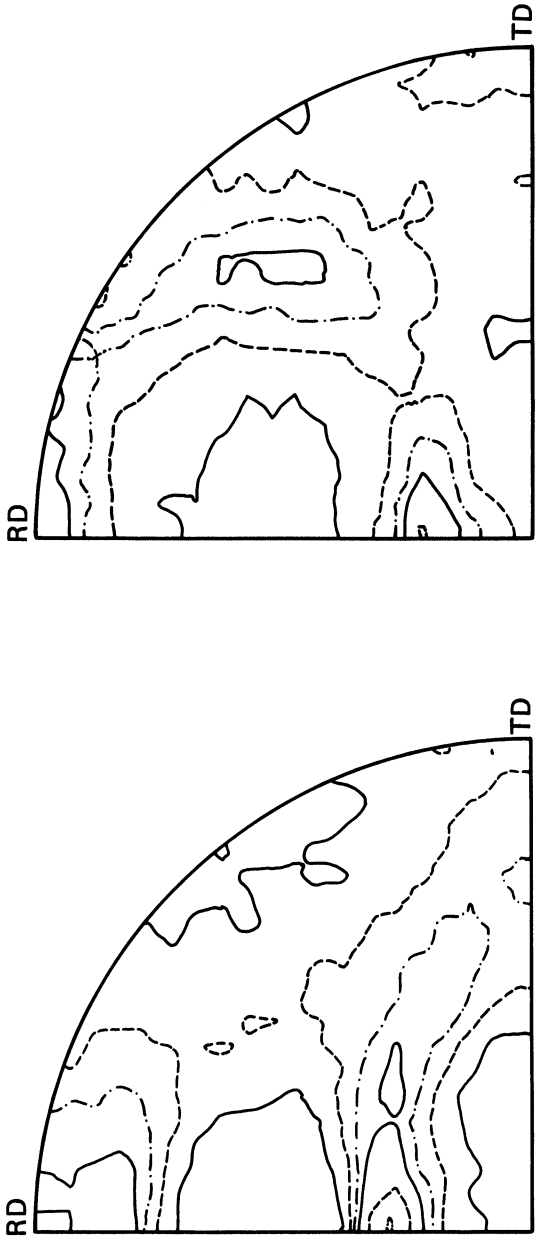

FIGURE 8 Simulated pole figures as in Figure 7, but now using the FC mode.

parameters are not very critical. For instance, the average magnitude of the random stress components is 0.33 times the average stress, but a magnitude of 0.25 times the average stress, which is the magnitude derived theoretically (Leffers, 1975), gives a fit which is almost as good. The average number of steps for which a given random stress is allowed to operate is such that the random stresses change about 10 times in the average grain during deformation to 40% reduction.

It is seen that both modes (RC and FC) produce quite good simulation of the experimental texture—not only for the shape of the maxima and minima but also for the numerical values of the pole densities. Some trends are best reproduced by one model, some by the other. In the {111} pole figure the position of the maximum close to ND on the ND–RD line is best reproduced by the FC mode, whereas the conditions close to RD are best reproduced by the RC mode. The {200} pole figure is best reproduced by the RC mode.

Figures 9–10 show the experimental and the simulated pole figures for Cu II. For Cu II we only show the simulated pole figures for the RC mode; the relation between the RC and the FC mode is the same as for Cu I.

Figure 11 shows simulated pole figures for 40% reduction with the RC mode starting with computer-generated random orientations. The pole figures in Figure 11 are very similar to those in Figures 7 and 10. Obviously Cu I and Cu II represents a case where the difference between the two textures and their deviation from random texture are insignificant for the development of deformation texture as reflected in the similarity between the two sets of experimental pole figures and the three sets of simulated pole figures.

Aluminium materials

Figures 12–14 show the experimental pole figures for fine-grained aluminium rolled to 50% reduction and the corresponding computer-simulated pole figures for the RC and FC mode with the random stress parameters which give the best fit to the experimental pole figures. The random stress parameters (also for coarse-grained aluminium, see below) turn out to be the same as the ones found

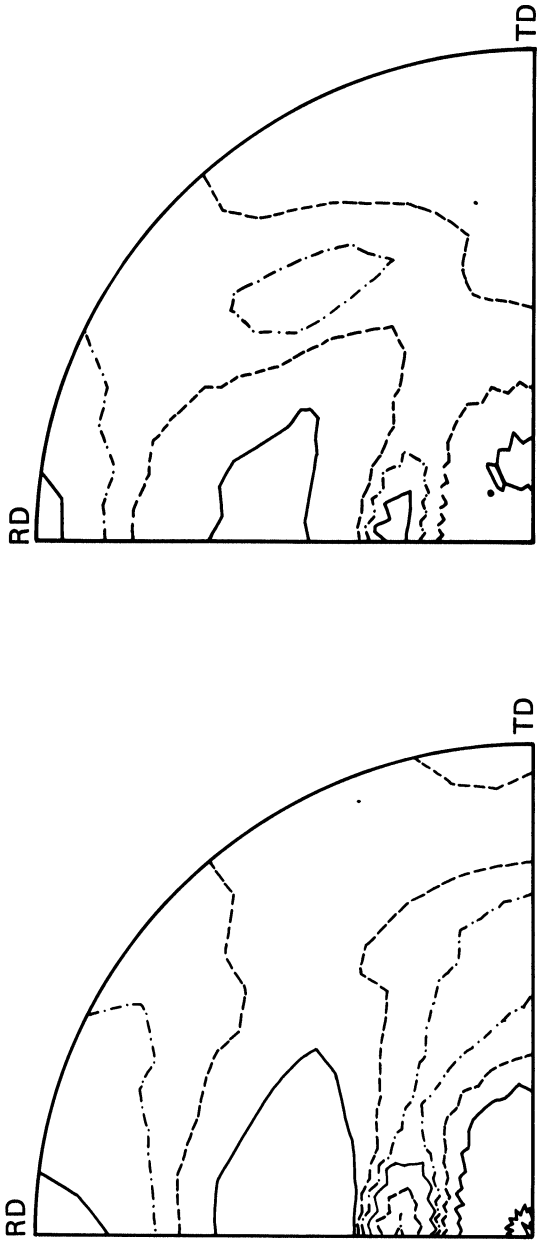

FIGURE 9 Experimental pole figures for Cu II rolled to 37% reduction.

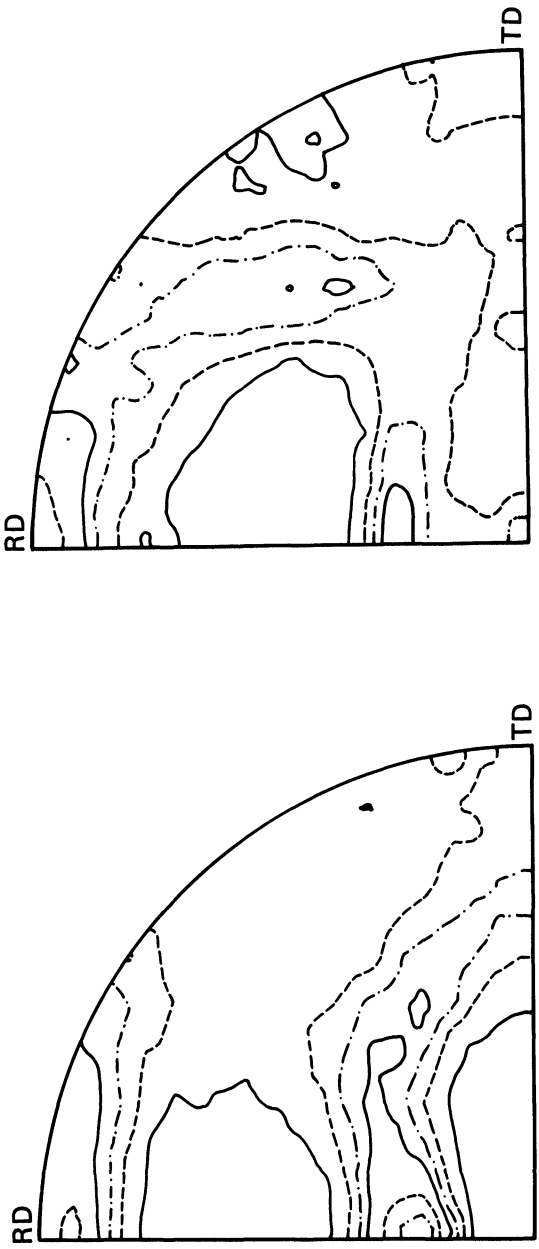

FIGURE 10 Pole figures corresponding to those in Figure 9, simulated with the RC mode starting with an orientation distribution representing the starting texture of Cu II. Reduction 37% as in Figure 9.

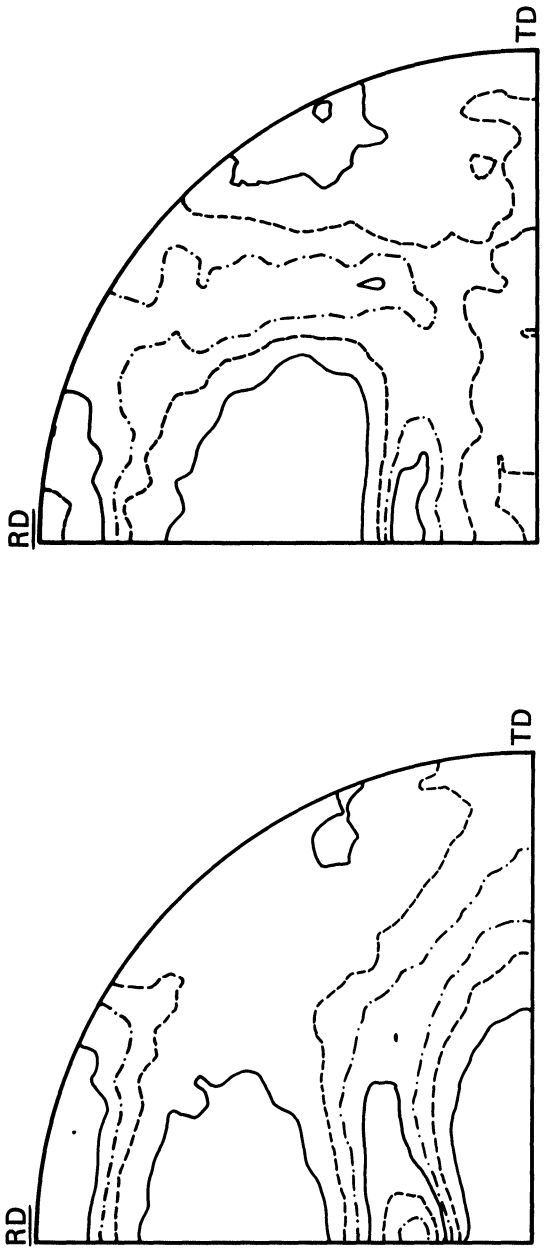

FIGURE 11 Pole figures simulated with the RC mode starting with (10,000) random orientations; 40% reduction.

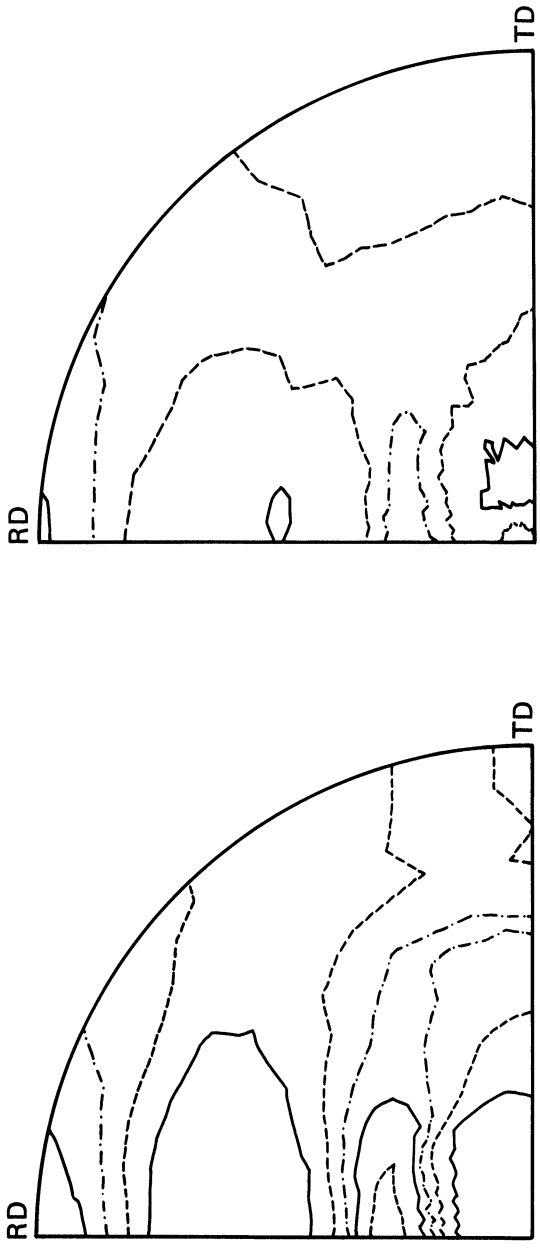

FIGURE 12 Experimental pole figures for fine-grained aluminium rolled to 50% reduction.

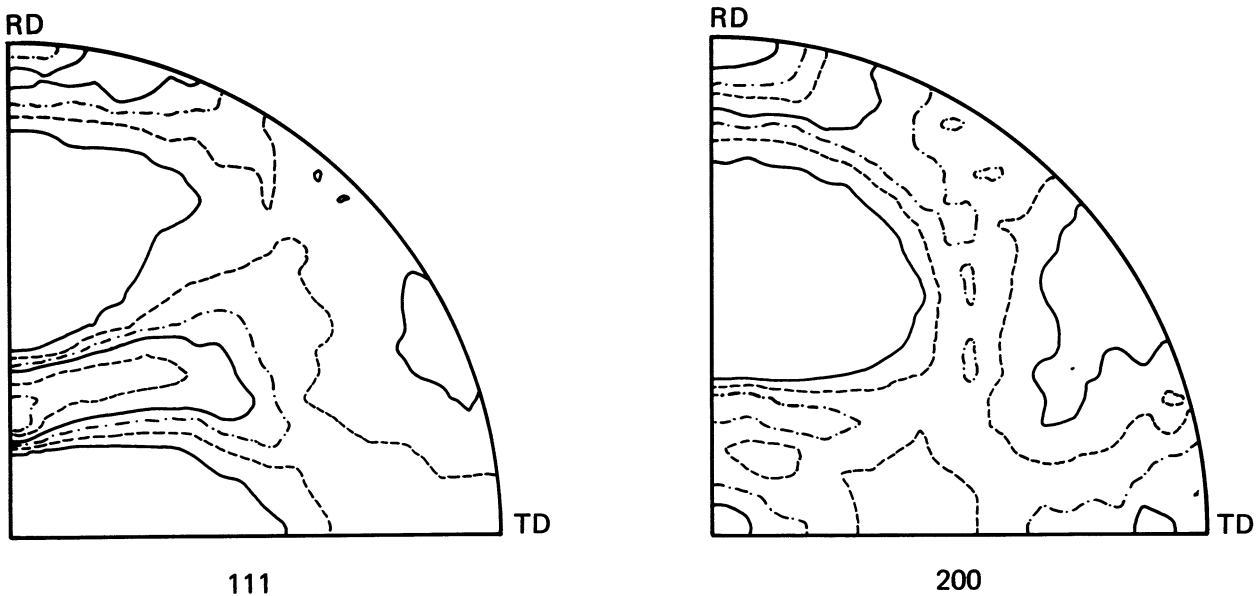

FIGURE 13 Pole figures corresponding to those in Figure 12, simulated with the RC mode starting with an orientation distribution representing the starting texture of fine-grained aluminium. Reduction 50% as in Figure 12.

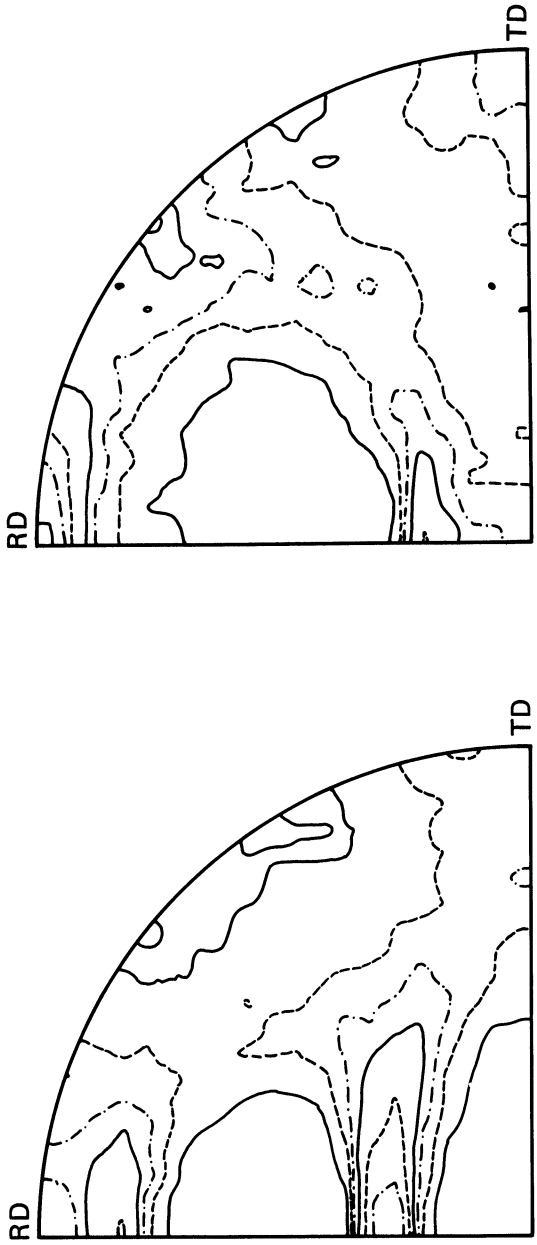

FIGURE 14 Simulated pole figures as in Figure 13, but now using the FC mode.

best suited for the copper materials. For aluminium we found, as we did for copper, that the simulated pole figures do not depend very critically on the values of the random stress parameters. Figures 15–16 show the experimental pole figures for coarse-grained aluminium rolled to 50% reduction and the corresponding simulated pole figures for the RC mode.

Comparison of Figures 12, 13 and 14 shows that it is difficult to say whether the RC or the FC mode produces the best fit to the experimental texture (the same problem exists for coarse-grained material for which the simulated pole figures for the FC mode are not shown). In the following, we shall discuss the similarities and dissimilarities between the experimental aluminium textures and the simulated textures in terms of textures simulated with the RC mode, but the conclusions would be basically the same if we used the FC mode.

For comparison with the pole figures for non-random starting materials in Figures 12–16 we show the simulated pole figures for the RC mode and the same random stress parameters (still 50% reduction) with texture-free starting material in Figure 17. It is evident that both the experimental and the simulated pole figures in Figures 12–16 deviate significantly from the pole figures for texture-free starting material in Figure 17. And it is evident that the main trend in the deviation is found in all the pole figures in Figures 12–16, viz. a predominant fibre-like texture component with ⟨100⟩ close to RD (high density of {200} poles close to RD and absence of clear density maxima in the remainder of {200} pole figure). This main trend is obviously a consequence of the initial texture which is reproduced in the simulated texture.

It is also clear that the fibre component is more predominant in the experimental texture for coarse-grained material than in that for fine-grained material (as already reflected in Figure 5). Even this difference is qualitatively reproduced in the simulated textures, which means that it is to some extend a consequence of the difference in starting texture.

However, the difference between the experimental textures for the fine-grained and the coarse-grained material is far more pronounced than the difference between the corresponding simulated textures, which shows that there is a genuine effect of grain size on texture. In particular one notes the formation of a distinct

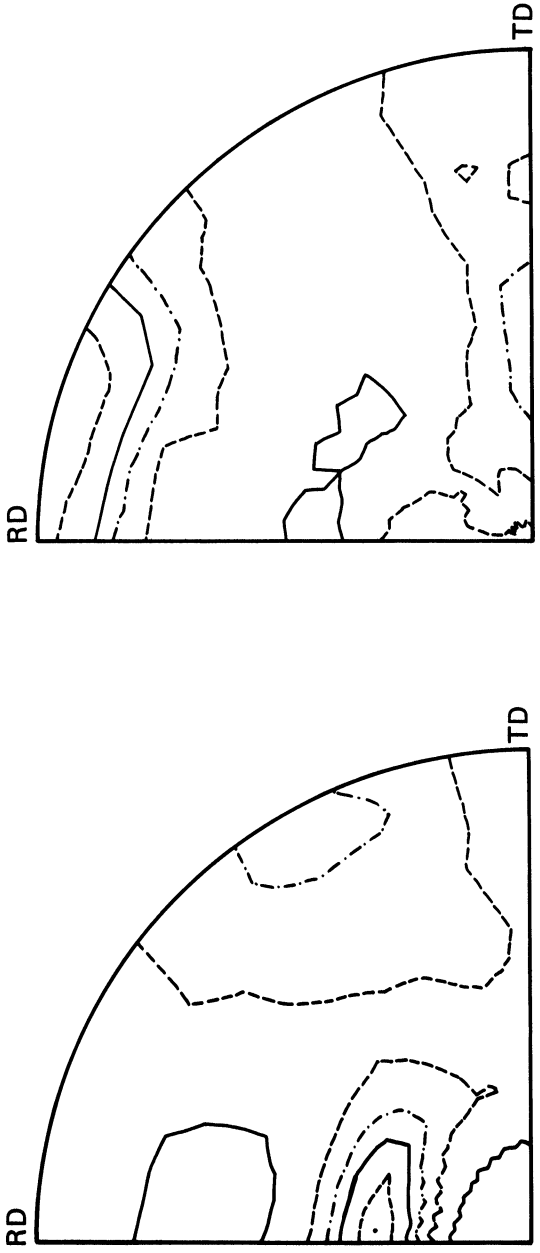

FIGURE 15 Experimental pole figures for coarse-grained aluminium rolled to 50% reduction.

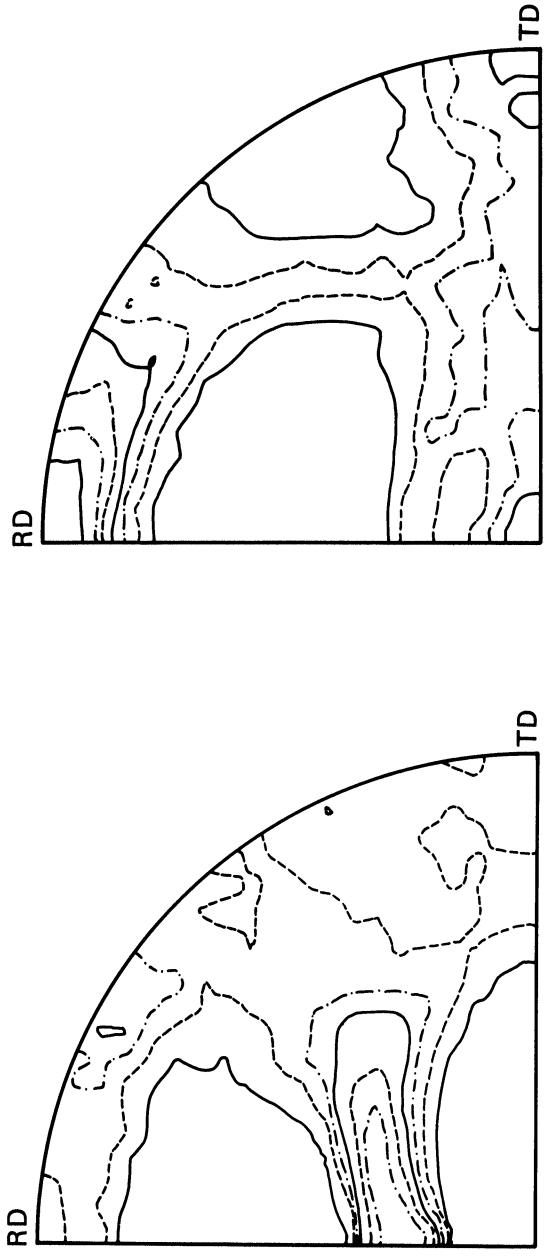

FIGURE 16 Pole figures corresponding to those in Figure 15, simulated with the RC mode starting with an orientation distribution representing the starting texture of coarse-grained aluminium. Reduction 50% as in Figure 15.

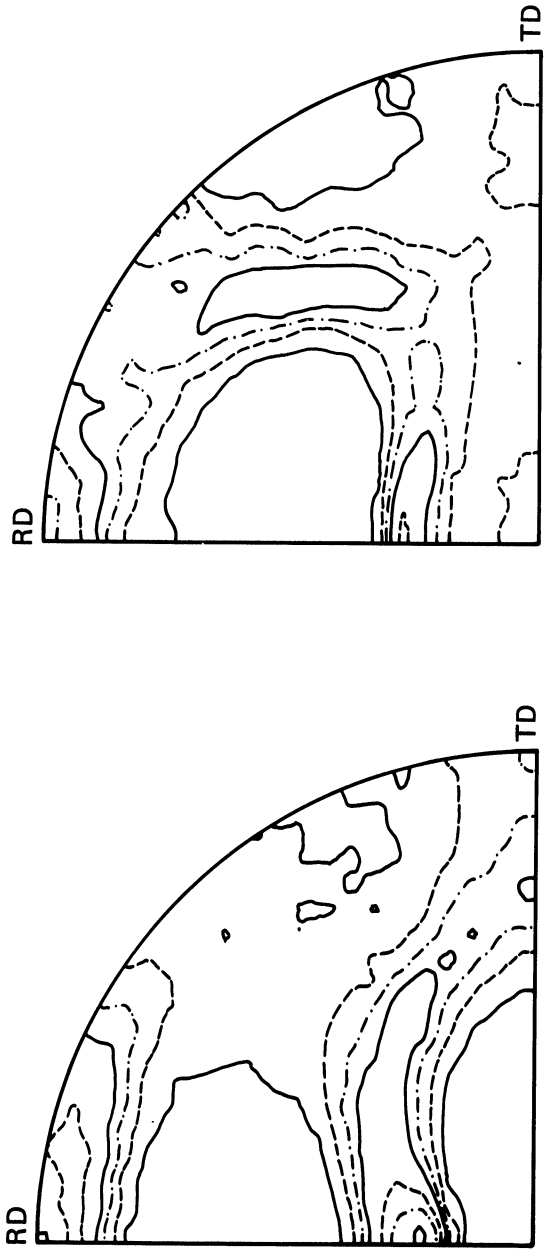

FIGURE 17 Pole figures simulated with the RC mode starting with (10,000) random orientations; 50% reduction.

maximum in orientation density in the Goss ($\{110\}\langle 001\rangle$) orientation in the coarse-grained material which is not found in fine-grained material (Figures 4, 12 and 15); this maximum does not develop in any of the simulated textures. There is also a great difference in the rate of change with strain of the fraction of fibre texture between fine-grained and coarse-grained material, as illustrated in Figure 5, which is not reflected in the simulated textures (the simulated development in fibre fraction is very similar for fine-grained and coarse-grained material).

Simulated texture for high degrees of reduction

Normally the main concern about computer models for texture simulation is their capability to simulate the textures of initially texture-free materials for high degrees of reduction. In this subsection we shall consider out models from this angle. The capacity of our simulation program used in the RC mode to reproduce the experimental copper texture at high degrees of reduction has already been demonstrated (with slightly different random stress parameters, with far fewer orientations/grains and with less sensitive means of comparison between experimental and simulated textures) in several earlier works (e.g. Leffers (1968, 1969b), Bunge and Leffers (1971)). Figure 18 shows the simulated pole figures for 94% reduction with the RC mode and the random stress parameters described earlier and with a starting material with random orientations. Comparison with pole figures for the fully developed copper texture quoted in literature shows that the pole figures in Figures 18 represent a rather good simulation, also with respect to the numerical values of the pole densities. However, there is one clear discrepancy between the simulated texture for high reduction and the experimental copper-type texture: as shown in Figure 18 the simulated texture has a rather strong fibre-texture component with $\langle 100\rangle$ parallel to the rolling direction; 17% of the grains have $\langle 100\rangle$ within 15° from RD, which is much stronger than the corresponding component in the experimental copper-type texture. The same discrepancy but somewhat less pronounced is observed for the RC mode without random stresses (pole figures not to be shown); for these conditions the density of $\{200\}$ poles close to RD is 4 (it is 9 in Figure 18), corresponding to a volume fraction of 7% for the

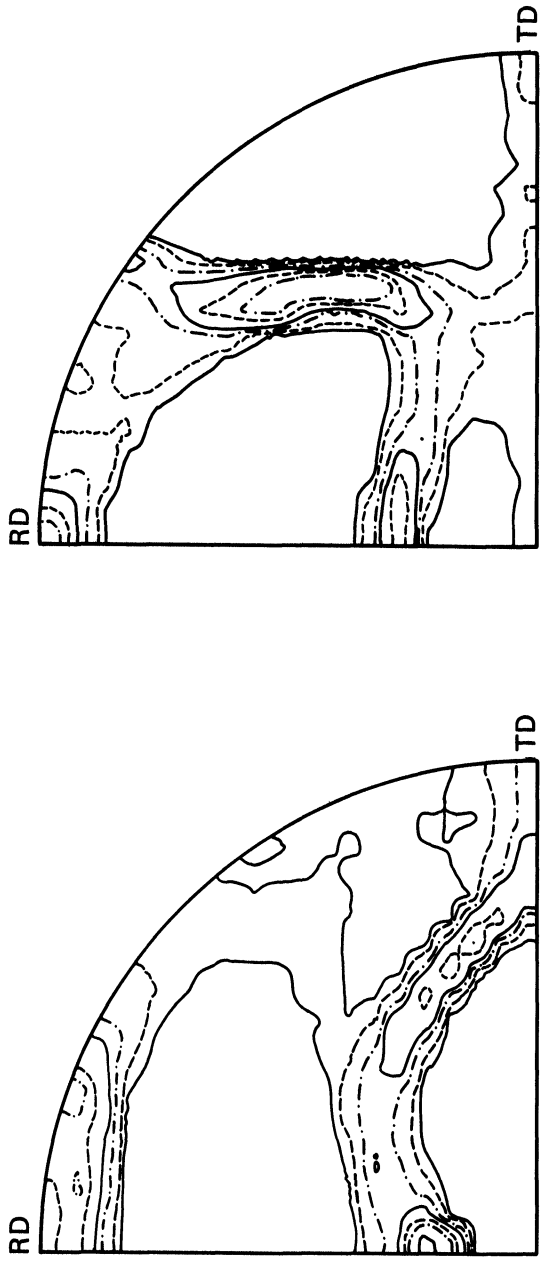

FIGURE 18 Pole-figures simulated with the RC mode starting with (5000) random orientations; 94% reduction. The "wrinkles" on some of the contour lines come from the original subdivision of the pole figures into areas with constant pole density; for very sharp textures this subdivision is too coarse.

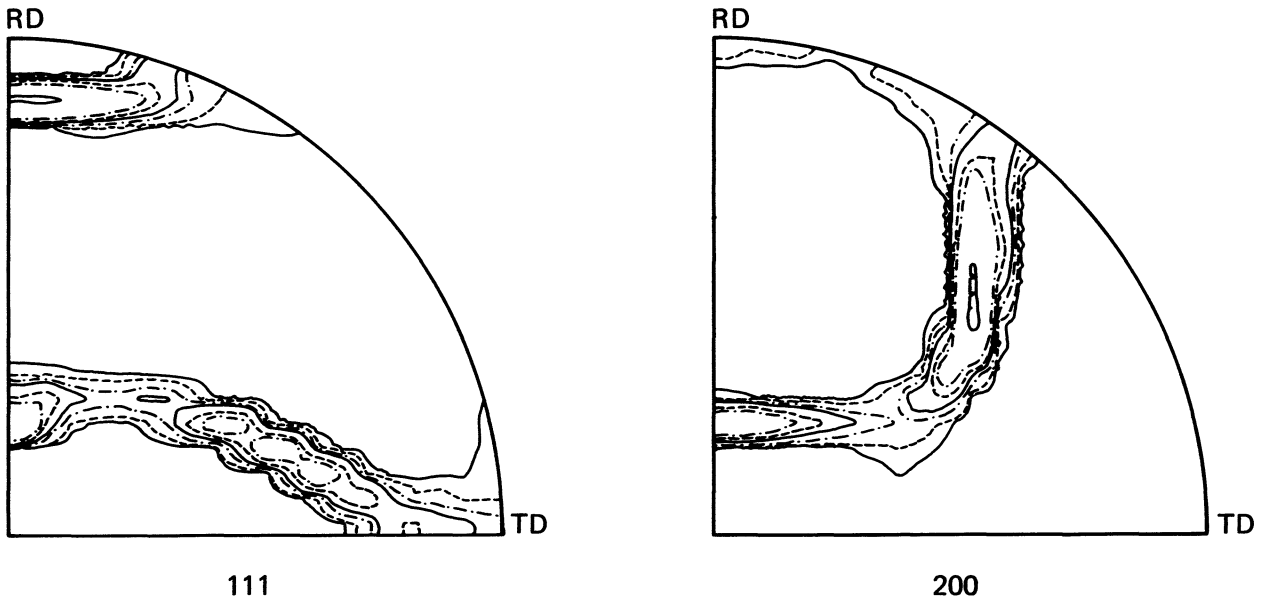

FIGURE 19 Pole figures simulated with the FC mode starting with (5000) random orientations; 94% reduction. Wrinkles as in Figure 18.

⟨100⟩ fibre component. As shown in Figure 19 the FC mode with random stresses does not produce excessively high pole densities near RD in the {200} pole figure (but they are still higher than those observed experimentally). On the other hand, the FC mode is clearly inferior to the RC mode in all other respects for the high degrees of reduction.

Going back to the simulated copper pole figures for the lower degrees of reduction one notes that the RC mode tends to produce a rather high density of {200} poles near RD also at these reductions. However, the corresponding experimental pole figures also have a quite high density of {200} poles near RD.

For copper there is no doubt that the texture for high degrees of reduction is best simulated with the RC mode (starting with random orientations). For aluminium it has been argued (e.g. van Houtte, 1981) that the texture for high degrees of reduction is closer to that obtained by simulation with the FC mode. However, if one compares the simulated pole figures in Figures 18–19 with the experimental pole figures for the fully developed aluminium texture quoted in the literature (for supposedly texture-free starting materials), there is no doubt that the RC mode comes closest to the aluminium pole figures, both in the general shape and in the numerical values of the pole densities (even though, as mentioned above, the density of {200} poles close to RD is less unrealistic for the FC mode). By comparison with copper one does, though, observe the trend suggested by van Houtte: a certain change in general shape in the direction of the FC mode.

We shall return to the degree of similarity between experimental and simulated textures in the discussion.

DISCUSSION

The copper materials represent the case of rather weak starting textures. With the accuracy with which our models at present can simulate the texture development we cannot in the simulations (at the level of 40% reduction) detect any experimentally significant effect of the starting textures in the two materials (experimentally significant in the sense that it is reflected in the experimental textures). As a matter of fact one would normally consider the two materials to be rather close to the ideal of random starting materials

even though there are distinct textures in both materials. This means that our sensibility limit is in agreement with normal experimental practice.

In the aluminium materials, on the other hand, the starting textures have very significant effects on the simulated textures: the textures simulated with the experimental initial textures as starting conditions developed a predominant $\langle 100 \rangle$ fibre component corresponding to that found in the experimental textures. Furthermore, the simulated textures do reflect the relatively small difference in initial texture between fine-grained and coarse-grained material: the fibre component is strongest in the texture simulated on the basis of the initial texture of the coarse-grained material, which corresponds to the experimental observations.

However, there are also differences between the experimental textures of the two aluminium materials that the simulated textures do not reproduce, for instance the presence in the coarse-grained material of a distinct peak in orientation density near $\{110\}\langle 001 \rangle$, which is not observed in the fine-grained material. This $\{110\}\langle 001 \rangle$ peak is not found in any of the simulated textures. The obvious conclusion is that the grain size has an effect on texture development in the aluminium materials. The same conclusion was reached by Liu and Alers (1973) for tin bronze, by Leffers (1974) and Öztürk, Kallend and Davies (1981) for copper and brass and preliminarily by Hansen *et al.* (1985) for the present aluminium materials, but these works did not include any systematic investigation of the possible effect of the initial textures.

We have thus demonstrated that the present procedure fulfils the aim specified in the introduction, viz. to reveal whether an apparent anomaly in texture development is caused by the initial texture or by some other characteristic of the material, in casu the grain size. By identifying a grain-size effect we obviously pinpoint a shortcoming of our texture-simulation models: they do not account for this grain-size effect.

Even apart form the difference in texture between fine-grained and coarse-grained material that our models do not reproduce, one notes that the aluminium materials do not show the same high degree of similarity between experimental and simulated textures as the copper materials. This may be because the models are basically better suited for the simulation of the behaviour of copper. But there

is another possible explanation worth considering: our models may be more realistic for some orientations and less realistic for others (in our case more realistic for the weak initial textures of the copper materials than for the initial textures of the aluminium materials). This possibility is supported by the simulated textures for high degree of reduction: the RC mode with random stresses, which produces a very good simulation of most of the characteristic trends of the fully developed copper texture, seriously overestimates the ⟨100⟩ fibre texture component (and the sample applies to the RC mode without random stresses even though the overestimate is less drastic). Exactly the ⟨100⟩ fibre component is also a predominant texture component in the aluminium materials, and hence the indication is that it is a difficult component to deal with from a texture-simulation point of view.

With procedures like the ones described in the present work we can abandon the attitude which has been practically universal up to now that texture simulation should only deal with initially texture-free materials. This means that we get a broader experimental basis for the texture-simulation work. New investigations on this basis may lead to the discovery of a number of "non-trivial" effects of initial texture which would require modification of our models and hence contribute to an improved understanding of the plastic deformation of polycrystals.

CONCLUSIONS

We describe a computer procedure for the simulation of the development of rolling texture in materials with non-random starting textures.

Such a procedure allows us to investigate details in texture development (particularly in the early stages) which would otherwise have questionable significance. We have used the procedure to demonstrate an effect of grain size on the texture development in aluminium.

We suggest that investigations along the line of the present work can contribute to an improved understanding of the plastic deformation of polycrystals by revealing some of the shortcomings of the present models.

References

Bunge, H. J. (1969). *Mathematische Methoden der Texturanalyse.* Akademie-Verlag, Berlin.
Bunge, H. J. and Leffers, T. (1971). *Scripta Metall.* **5,** 143.
Hansen, N., Bay, B., Juul Jensen, D. and Leffers, T. (1985). *Strength of Metals and Alloys.* Eds. McQueen *et al.* Pergamon Press, Oxford, vol. 1, 317–322.
Hansen, J., Pospiech, J. and Lücke, K. (1978). *Tables for Texture Analysis of Cubic Crystals.*. Springer-Verlag, Berlin 22–28.
van Houtte, P. (1981). ICOTOM 6. Ed. S. Nagashima. The Iron and Steel Institute of Japan, Tokyo 428–437.
Juul Jensen, D., Hansen, N., Kjems, J. and Leffers, T. (1984). *Microstructural Characterization of Materials by Non-Microscopical Techniques.* Eds. Hessel Andersen *et al.* Risø National Laboratory 325–332.
Juul Jensen, D. and Kjems, J. (1983). *Textures and Microstructures* **5,** 239.
Kallend, J. S. and Davies, G. J. (1972). *Phil. Mag.* **25,** 471.
Leffers, T. (1968). Risø Report No. 184.
Leffers, T. (1969a). *Z. Metallkde.* **60,** 535.
Leffers, T. (1969b). *Textures in Research and Practice.* Eds. Grewen and Wassermann. Springer-Verlag, Berlin 120–129.
Leffers, T. (1973). Risø Report No. 283.
Leffers, T. (1974). *Met. Trans.* **5,** 2110.
Leffers, T. (1975). Risø Report No. 302.
Liu, Y. C. and Alers, G. A. (1973). *Met Trans.* **4,** 1491.
Öztürk, T., Kallend, J. S. and Davies G. J. (1981). ICOTOM 6. Ed. S. Nagashima. The Iron and Steel Institute of Japan, Tokyo 507–518.
Sundberg, R. (1968). *Z. Metallkde.* **59,** 202.
Taylor, G. I. (1938). *J. Inst. Metals* **62,** 307.
Tome, C., Canova, G. R. Kocks, U. F., Christodoulou, N. and Jonas, J. J. (1984). *Acta Metall.* **32,** 1637.